Chalcogenide Letters Vol. 10, No. 6, June 2013, p. 197 - 207

THE FORMATION AND CHARACTERIZATION OF BISMUTH SELENIDE FILMS ON PT ELECTRODE FROM CHOLINE CHLORIDE – MALONIC ACID IONIC LIQUID

F. GOLGOVICI, T. VISAN, M. BUDA*
Faculty of Applied Chemistry and Materials Science, University "Politehnica" of Bucharest, 1-7 Polizu Street, 011061 Bucharest, Romania

Bismuth selenide electrodeposition on platinum in a ionic liquid based on choline chloride and malonic acid mixture at 35-65^{0}C is reported. The electrode processes during Bi_2Se_3 electrodeposition/dissolution were investigated by cyclic voltammetry. It is suggested that selenium underpotential deposition may take place before Bi^{3+} and Se^{4+} co-reduction, so that bismuth selenide deposition may occur on a selenium underlayer. An additional overpotential deposition of Bi metal was evidenced at more negative potentials.
Bi_2Se_3 films were grown on Pt by electrolysis under controlled potential and were characterized by AFM microscopy as well as by potentiodynamic polarization curves as corrosion tests.

(Received May 13, 2013; Accepted June 18, 2013)

Keywords: Bismuth selenide, Ionic liquid, Electrodeposition, Choline chloride- malonic acid mixture

1. Introduction

Dibismuth triselenide Bi_2Se_3 is a V_2VI_3 -type semiconductor with quite similar properties to dibismuth tritelluride, with a narrow band gap, estimated theoretically to be ~0.35 eV and experimentally somewhere between 0.2 – 0.3 eV. Its electronic structure and properties (especially thermoelectric and photoconductive performances) have been the subject of numerous studies [1 – 7] in which Bi_2Se_3 films were prepared using various non-electrochemical techniques. As these studies show, Bi_2Se_3 films are of continued interest for investigators from the point of preparation and characterization in order to test their suitability for a particular and desired application in thermoelectricity, for construction of optoelectronic, photosensitive and IR photography devices, as well as decorative and solar selective coatings.

Electrochemical deposition has also been extensively applied to obtain high quality thin films [6 – 17] or nanowires [18] of Bi_2Se_3 semiconductor. In most cases aqueous acidic baths are used, with non-aqueous baths being rather the exception (one containing dimethylsulphoxide as solvent is described in ref. [9]). Over the past decade, room temperature ionic liquids based on choline chloride (ChCl) have been employed in the electrodeposition of metals and semiconductors, since they exhibit several advantages over the conventional elctrolytes, including a wide electrochemical window, low vapor pressure and good thermal stability. As part of the work developed in our group and focused on semiconductor compounds [19 – 24], we report here studies concerning the electrodeposition of Bi_2Se_3 from choline chloride (ChCl) – malonic acid (MA) mixtures; to the best of our knowledge, the electrodeposition of Bi_2Se_3 from these types of ionic liquids compound has not been investigated.

*Corresponding author: mihai@catedra.chfiz.pub.ro

2. Experimental

The ionic liquid was prepared as an eutectic mixture of 1:1 molar ratio of choline chloride (ChCl, 99%, Aldrich) with malonic acid (MA, 99%, Aldrich), both reagents being used as received. Bi_2O_3 and SeO_2 (Alfa Aesar) were used as precursors for the ionic species of bismuth and selenium in solution. The molarities were calculated using density values determined in [25]. All electrochemical experiments were performed using an AUTOLAB PGSTAT 12 EcoChemie potentiostat driven by a PC computer. A platinum sheet (0.5 cm^2) was used as working electrode, whereas the auxiliary electrode was a platinum mesh. A silver wire immersed in separate compartment filled with working electrolyte containing bismuth and selenium ions was used as quasi-reference electrode [21]. The Pt working electrode was polished with alumina paste, rinsed and dried before every measurement. The cyclic voltammograms were recorded at various scan rates from 1 to 100 mVs^{-1}.

The deposition of Bi_2Se_3 films on Pt was carried out with potentiostatic control; all electrolyses were performed using a ChCl+MA ionic liquid containing 5 mM Bi_2O_3 and 7.5 mM SeO_2, 5 – 15 min time duration at -0.15 V and -0.2 V polarization and 50^0C or 65^0C temperature. After electrodeposition the samples were again rinsed with water and dried.

Film morphology was studied using AFM microscope (A.P.E. Research). The corrosion studies were performed employing a specially designed three-electrode cell [26]. Inside the corrosion cell, filled with 0.5 M NaCl aqueous solution, the electrode covered with Bi_2Se_3 film was placed horizontally at the bottom, having an exposed area of 0.64 cm^2. A platinum plate was used as auxiliary electrode and a conventional Ag/AgCl-3M KCl electrolyte electrode (Metrohm) was the reference electrode. Current-potential polarization curves in potentiodynamic conditions (3 mVs^{-1} scan rate) were carried out at room temperature starting from 350 mV potential more negative than stabilized open-circuit potential (OCP) and scanning up to 350 mV more positive potential from OCP.

3. Results and discussion

3.1. Studies of electrode processes using cyclic voltammetry

Cyclic voltammograms recorded comparatively on Pt at 50^0C for ChCl – MA ionic liquid containing Bi^{3+}, Se^{4+} and Bi^{3+} + Se^{4+} ionic species, respectively, are shown in Figure 1. On the cathodic branch (Fig.1a) the onset of a large current plateau at +0.3 V with few hundred microampers in amplitude is apparent, corresponding to bismuth underpotential deposition (UPD). The shoulder between -0.2 and -0.3 V, with an average current density of 3 $mAcm^{-2}$, can be attributed to the bulk, overpotential deposition (OPD) of bismuth. Below -0.3 V the continuous increase of current is due to solvent-related cathodic processes, either reduction of choline cation or hydrogen evolution. Two oxidation peaks are evident on the anodic branch at +0.1 V and +0.5 V. These peaks are generally attributed to the dissolution of UPD and OPD Bi respectively [14, 27] but stepwise oxidation of Bi through a Bi^+ intermediate cannot be ruled out [28, 29].

On the voltammogram for selenium deposition/dissolution (Fig.1b) a less visible plateau for UPD of Se is first recorded starting from +0.4 V potential. The onset of Se OPD Se is noticed for potentials below +0.1 V. Returning scans shows a single peak, attributed to the dissolution of the selenium deposit.

Fig.1c illustrates the successive reduction processes during Bi_2Se_3 deposition on Pt, which is somewhat a combination between previously discussed electrode processes involving Bi and Se elements. Thus, the less visible current plateau with the onset at +0.4 V corresponds to a few layers of Se which may be deposited at these most positive potentials. Next, the clear cathodic peak followed by its short limiting current (in a potential range from -0.15 V to -0.18 V) represents Bi_2Se_3 deposition. We notice that the reduction process for depositing Bi_2Se_3 compound takes place at potentials quite similar to that shoulder of metallic bismuth deposition (see Fig.1a), but with lower peak current for binary compound. Extending the scan to more negative potentials the current increases again owing to a supplementary process of Bi deposition; this accompanies

Bi_2Se_3 deposition and results in an increased content in Bi metal of deposit, similar to Bi_2Te_3 [30]. During anodic scan, the oxidation processes are exactly in an inverse order: the sharp peak at +0.1 V is typically for oxidation of a metal (bismuth) to its ions (Bi^{3+}) as a stripping process on Pt; the broad peak at +0.28 V represents Bi_2Se_3 dissolution producing both Bi^{3+} and Se^{4+}ions; the last broad peaks (in the range from +0.45 V to +0.55 V) are attributed to selenium dissolution resulting Se^{4+} ions only.

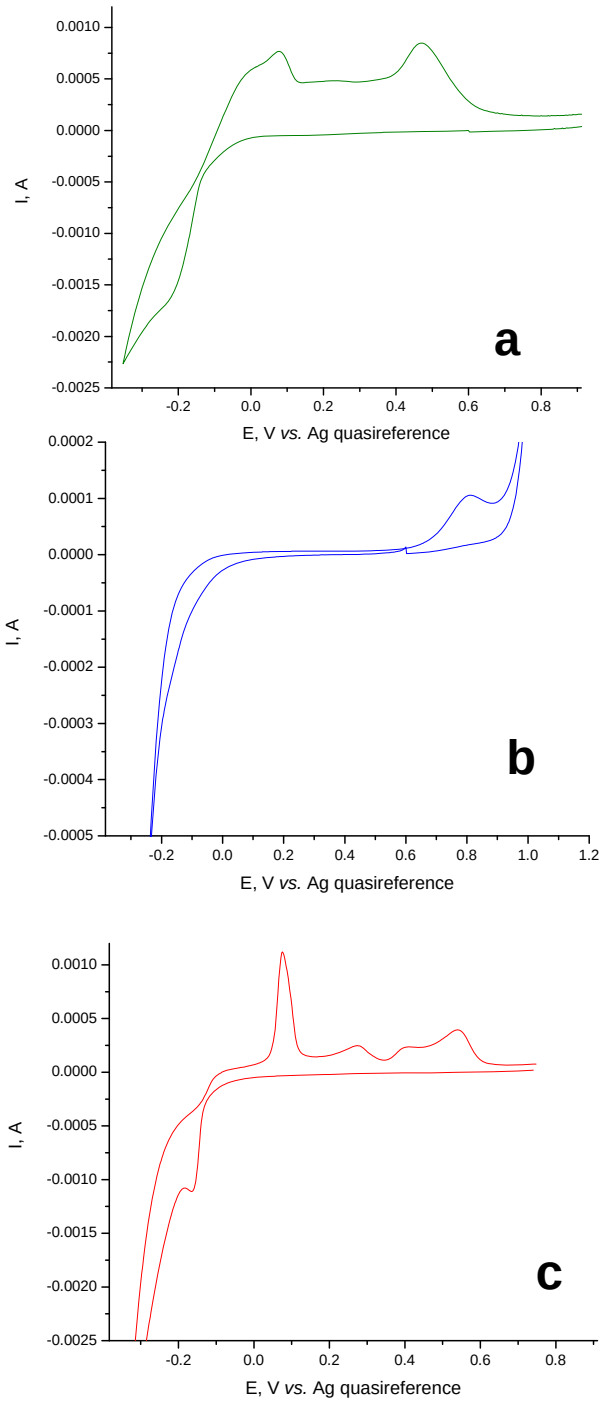

Fig. 1. Comparative cyclic voltammograms on Pt (0.5 cm^2) for deposition/dissolution of Bi, Se and Bi_2Se_3 using choline chloride – malonic acid ionic liquid; temperature 50^0C, scan rate 2 mVs^{-1}. Concentrations of dissolved precursors: 5 mM Bi_2O_3 (a);5 mM SeO_2 (b); 5 mM Bi_2O_3 + 5 mM SeO_2 (c)

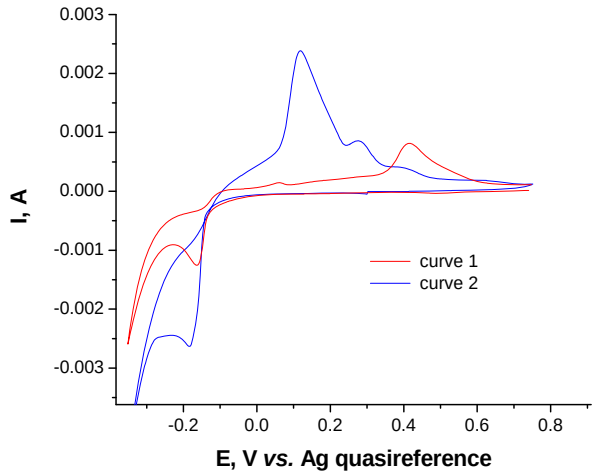

Fig. 2. Cyclic voltammograms on Pt for deposition/dissolution of Bi_2Se_3 using choline chloride – malonic acid ionic liquid; temperature 50^0C, scan rate 5 mVs^{-1}. Concentrations of dissolved precursors: 5 mM Bi_2O_3 + 5 mM SeO_2 (curve 1); 5 mM Bi_2O_3 + 7.5 mM SeO_2 (curve 2)

Figs. 2-4 show cyclic voltammograms related to Bi_2Se_3 film formation using various concentrations of precursors, scan rates and temperatures. Figure 2 illustrates similar cathodic and anodic branches for two different compositions of electrolyte by keeping constant the scan rate at 5 mVs^{-1}; the working temperature is the same as in Fig.1. On the cathodic scan one can notice a less visible current plateau corresponding to Se deposition, followed by a clear reduction peak attributed to Bi_2Se_3 film formation. For the system containing 5 mM Bi^{3+} + 7.5 mM Se^{4+} (curve 2) the current for this cathodic peak (-0.18 V) is substantially increased when compared to that for 5 mM Bi^{3+} + 5 mM Se^{4+} composition (curve 1), due to the higher concentrations of selenium. The potential shifts towards more negative values, while the current increases as the scan rate increases. Also, on the anodic branch of curve 2, all three oxidation peaks increase and shift to more positive potentials as the scan rate increases, compared to oxidation peaks on curve 1.

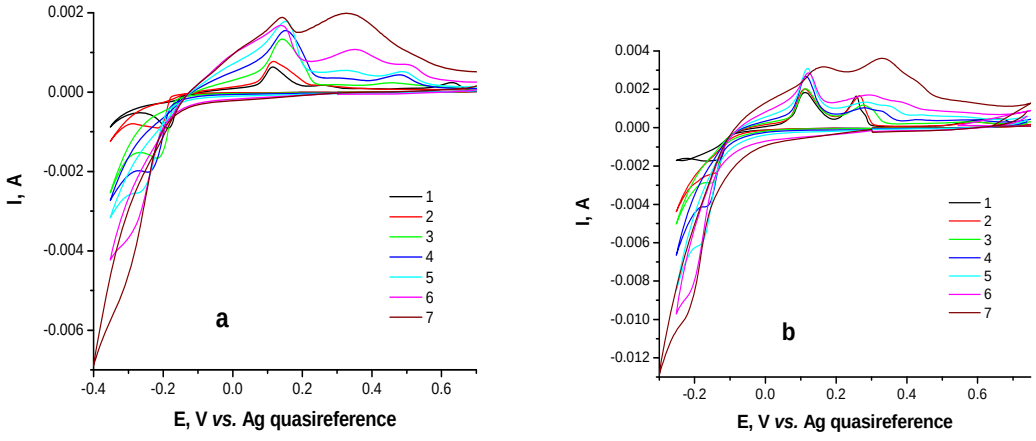

Fig. 3. Influence of changing scan rate upon cyclic voltammograms on Pt for deposition/dissolution of Bi_2Se_3 using choline chloride – malonic acid ionic liquid. Temperatures: 35^0C (a) and 65^0C (b). Scan rates: (1) 1; (2) 2; (3) 5; (4) 10; (5) 20; (6) 50 and (7) 100 mVs^{-1}. Concentrations of dissolved precursors: 5 mM Bi_2O_3 + 7.5 mM SeO_2

Fig. 3 illustrates the evolution of Bi_2Se_3 deposition/dissolution characteristics at various scan rates, whereas Figure 4 gives an example (1 mVs^{-1} constant scan rate) of the temperature

influence on the shape of voltammograms. One may notice that the stripping peak for Bi_2Se_3 (~0.28 V) increases significantly (compared to the one for Bi) as the temperature increases, suggesting a larger proportion of Bi_2Se_3 in the deposit at higher temperatures.

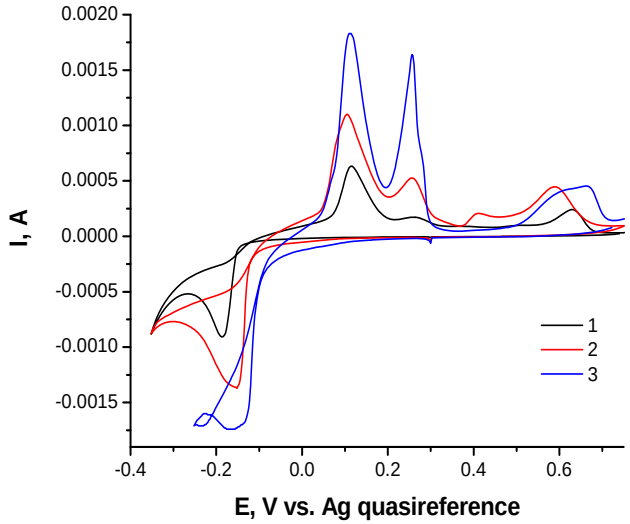

Fig. 4. Influence of changing temperature upon cyclic voltammograms on Pt at 1 mVs^{-1} scan rate for deposition/dissolution of Bi_2Se_3. Electrolyte: choline chloride – malonic containing
5 mM Bi_2O_3 + 7,5 mM SeO_2,. Temperatures: 35^0C (1), 50^0C (2) and 65^0C (3)

The linear dependences of cathodic peak current (i_p) with square root of scan rate ($v^{1/2}$) shown in Fig. 5a demonstrate the diffusion controlled kinetics of Bi^{3+} and Se^{4+} co-reduction process. However, a shift towards negative potentials for cathodic peak potential (E_p) of Bi_2Se_3 deposition with scan rate is noticed at both temperatures that means a degree of irreversibility from electrochemically point of view; this is confirmed by E_p - v linear dependences, showed in Fig. 5b.

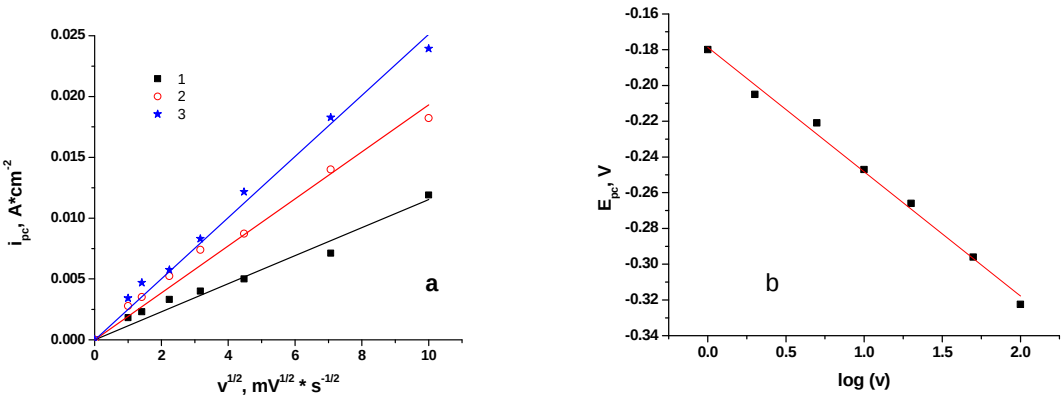

Fig. 5. Influences of changing scan rate upon peak currents (a) and peak potentials (b) of cyclic voltammograms shown in Figs.1-3 for cathodic deposition of Bi_2Se_3. Temperatures: 35^0C (1), 50^0C (2) and 65^0C (3)

The influence of changing the working temperature (35, 50 and 65^0C, respectively) upon peak current for deposition of Bi_2Se_3 may be also discussed. The cathodic peak of Bi_2Se_3 deposition increases with temperature, whereas only a small shift to more positive values is noticed for the peak potential.

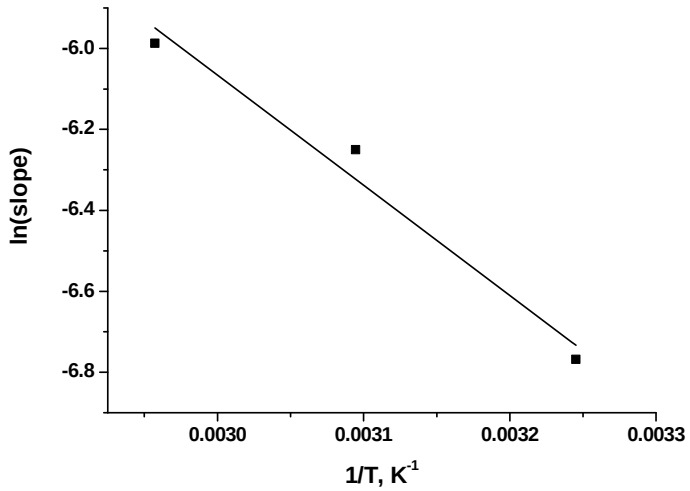

Fig. 6. Arrhenius semilogarithmic plots of the slopes in Fig. 5 with temperature for BiSe deposition on Pt with various scan rates; the electrolyte: choline chloride – malonic acid + 5mM Bi^{3+} + 7.5mM Se^{4+}

Since the slope of the $i_p - v^{1/2}$ (Fig. 5) depends on the square-root of the diffusion coefficient and neglecting all other (small) temperature dependence then an Arrhenius plot of the slope log should give one half of the activation energy for diffusion. From Figure 6 this value is calculated to be 22.6 kJ/mole, which gives for the diffusion activation energy a value of 45.2 kJ/mol. This value is nearly equal to the activation energy for viscous flow in the same ionic liquid (44.4 kJ/mole, [25]), which is to be expected since the diffusion coefficient should be inversely proportional to the solvent's viscosity.

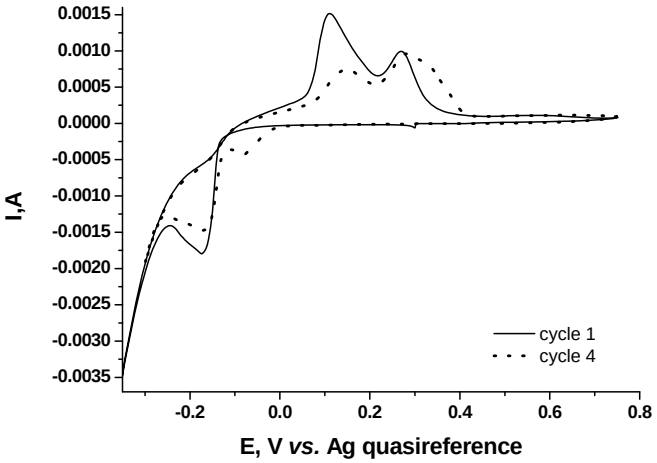

Fig. 7. Cyclic voltammograms on Pt for deposition/dissolution of Bi_2Se_3 using ChCl-MA + 5 mM Bi_2O_3 + 7.5 mM SeO_2 ionic liquid at 50^0C temperature, scan rate 2 mVs^{-1}: first cycle (solid line); fourth cycle (interrupted line)

Figures 7 and 8 show the multicyclic voltammograms recorded for deposition/dissolution of Bi_2Se_3 at 50^0C temperature. Figure 7 displays the first and the fourth cycles. Starting from the second cycle a pronounced cathodic peak occurs additionally at more positive potentials (peak potential at -0.075 V); as this peak becomes more pronounced as the Se concentration increses, it is suggested that it may relate to either selenium UPD or adsorption on a mixed Pt/Bi_2Se_3 surface. The main peak corresponding to Bi_2Se_3 co-deposition as well as the continuous increase of

cathodic current due to Bi metal formation at very negative potentials are well reproduced in all cycles with a small decrease of peak current of Bi_2Se_3. On the other hand, the first anodic peak (at +0.17 V potential) of Bi stripping is substantially diminished in the fourth cycle, suggesting a selective dissolution of Bi during continuous potential cycling.

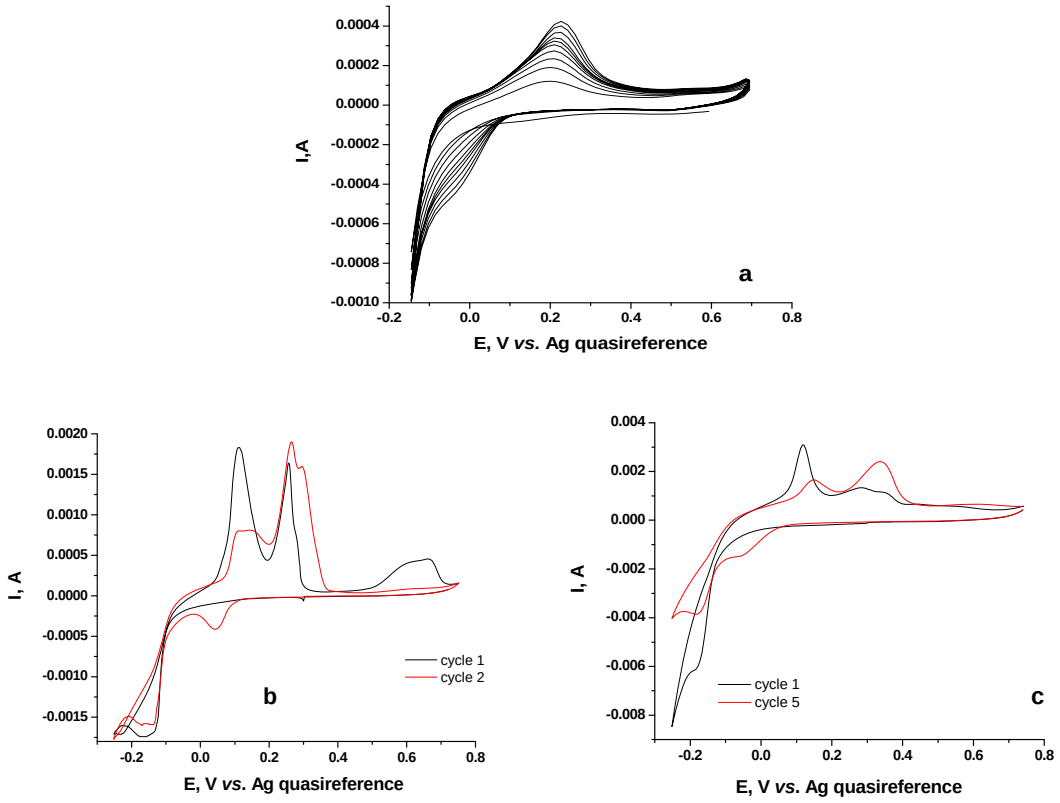

Fig. 8. Cyclic voltammograms on Pt for deposition/dissolution of Bi_2Se_3 at 65^0C temperature using two electrolytes: ChCl-MA + 5 mM Bi_2O_3 +5mM SeO_2 with $2mVs^{-1}$scan rate (a); ChCl-MA + 5 mM Bi_2O_3 + 7.5 mM SeO_2 with scan rates: 1 mVs^{-1}(b) and 20 mVs^{-1}(c). The number of cycles are indicated.

Fig. 8a displays ten successive voltammetric cycles of the Pt electrode in ChCl-MA + 5 mM Bi_2O_3 + 5 mM SeO_2 electrolyte at 65^0C (limited to -0.15 V only). The small peak attributed to Se UPD is clearly visible; extending the potential range in the cathodic direction (Figures 8c), results in a decrease to almost total disappearance of this small peak. Also, the relative height of the Bi_2Se_3 decreases significantly, while the Bi dissolution peak increases (Figures 8c), which is expected, since the deposit should contain more Bi as the cathodic limit is extended.

3.2. Characterization of Bi_2Se_3 films by atomic force microscopy

In order to characterize the surface smoothness of deposited films the measurements of atomic force microscopy were performed. Figures 9 and 10 exhibit some examples of bi-dimensional and three-dimensional AFM representation of a 5 μm × 5 μm area of as-deposited Bi_2Se_3 films deposited potentiostatically on Pt. Using ChCl+MA ionic liquid containing 5 mM Bi_2O_3 and 7.5 mM SeO_2, a film thickness around 2 μm was reached after 10 min electrolysis at 50^0C temperature. AFM images indicated the formation of ordered spherical nanoparticles of bismuth selenide. The morphology of Bi_2Se_3 sample from Fig. 9 is characterized by an average roughness (Ra) of 63.2 nm and a root mean square roughness (Rms) of 78.2 nm. Higher values were found for the second Bi_2Se_3 sample (Fig. 10), which has a Ra of 107.9 nm and a Rms of 137.3 nm, respectively.

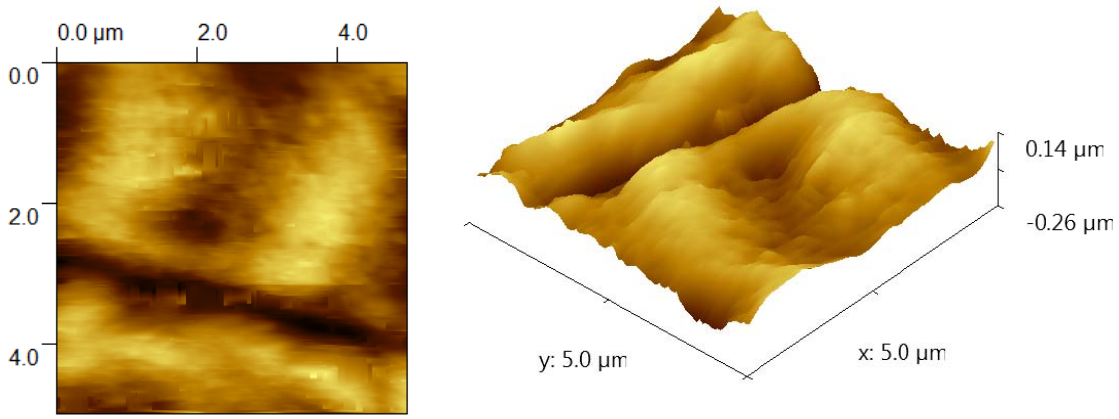

(a) (b)

Fig. 9. AFM micrographs as 2D image (a) and 3D image (b) of Bi_2Se_3 deposit on Pt electrode. Electrodeposition conditions: ChCl – MA ionic liquid containing 5mM Bi^{3+} + 7.5mM Se^{4+}as electrolyte, -0.2 V polarization potential (vs. Ag electrode), electrolysis time 10 min, 50^{0}C temperature.

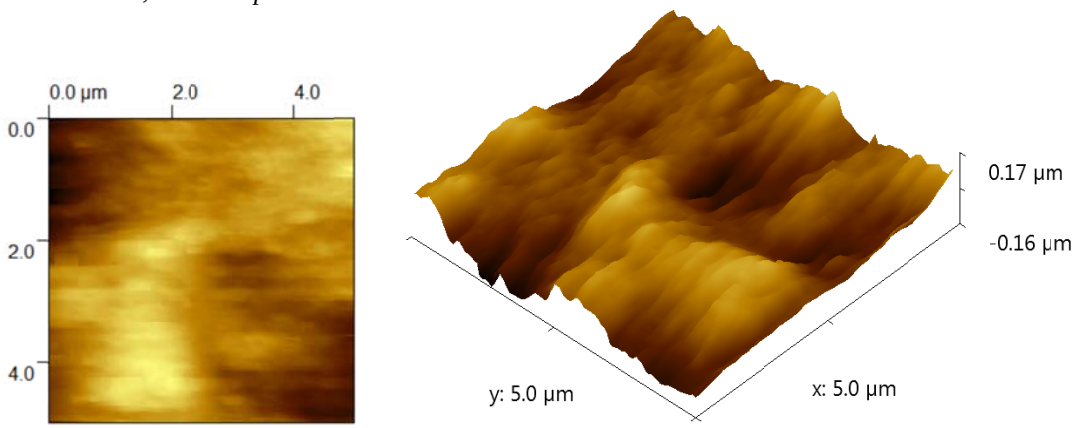

(a) (b)

Fig. 10. AFM micrographs as 2D image (a) and 3D image (b) of Bi_2Se_3 deposit on Pt electrode. Electrodeposition conditions: ChCl – MA ionic liquid containing 5mM Bi^{3+} + 7.5mM Se^{4+}as electrolyte, -0.15 V polarization potential (vs. Ag electrode), electrolysis time 10 min, 50^{0}C temperature.

3.3. Corrosion studies of Bi_2Se_3 films by polarization curves in 0.5M NaCl aqueous solution

Corrosion behavior of Bi_2Se_3 deposits in a stagnant 0.5M NaCl aqueous solution exposed to the atmosphere was studied by plotting the potentiodynamic polarization curves at room temperature. The investigated films were prepared in various electrolysis conditions of polarization potential, electrolysis time and temperature by keeping constant the composition of electrolyte (ChCl-MA + 5 mM Bi_2O_3 + 7.5 mM SeO_2). Before starting the corrosion test the working electrode was allowed to stabilize in the NaCl solution in order to reach a stable open circuit potential (OCP).

Figure 11 presents the polarization curves in semi-logarithmic coordinates (Tafel curves) obtained by starting the potential scan from the most cathodic potential and continuing the scan after the cathodic branch with the anodic one. The limiting current in the negative polarization domain is attributed to the cathodic reduction of dissolved atmospheric oxygen in the neutral NaCl

aqueous solution. More important is the anodic branch of polarization curve from which the corrosion behavior of bismuth selenide deposit in this aggressive medium may be interpreted. Its shape suggests for all grown Bi_2Se_3 films a first active domain of steep increase in anodic current indicating that the film undergoes dissolution without passivation. The second part is a short potential range with a limitation of anodic current which may be due to the barrier formed by corrosion products adsorbed on the electrode surface that possibly hinder the flow of anodic current. The final part of polarization, toward most positive potentials, shows a substantial increase of current indicating a partial dissolution of corrosion products that are now unable to protect Pt substrate.

Values of the corrosion current (i_{corr}) and corrosion potential (E_{corr}) were determined at the intercept of extrapolated linear parts (anodic and cathodic Tafel lines) of polarization curve. Also, the value of polarization resistance (R_p) was obtained as a slope of potential-current density curve (not shown) plotted within a potential domain ± 40 mV *vs.* E_{corr}, where a linear dependence is supposed to be valid. Values of i_{corr} were determined using the well-known equation [31]:

$$i_{corr} = \frac{R\,T}{n\,F\,R_p} \qquad (1)$$

where R, T and n have their usual meanings: universal gas constant, temperature, number of electrons involved in corrosion process, respectively. As an approximation, the n value was calculated taking into account the Bi_2Se_3 stoichiometry and considering 3 electrons for bismuth and 4 electrons for selenium.

All corrosion data calculated by both procedures utilized are listed in Table 1.

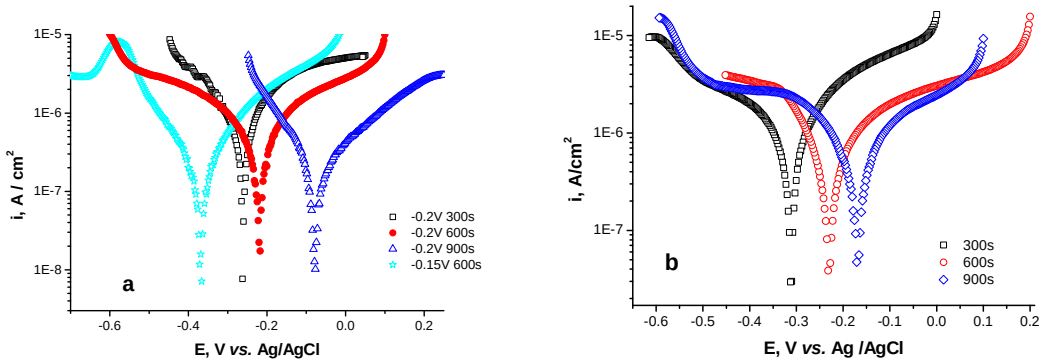

Fig. 11. Polarization curves plotted in potentiodynamic conditions for electrodeposited Bi_2Se_3 films grown on Pt from ChCl-MA + 5 mM Bi_2O_3 + 7.5 mM SeO_2 electrolyte at two temperatures: 50^0C (a) and 65^0C (b). Electrodeposition variables (-0.2V and -0.15 V potential, 5-15 min time duration) are indicated. Aqueous 0.5M NaCl solution.

In Table 1 the series of decreasing corrosion currents determined for Bi_2Se_3 films obtained at -0.2 V polarization indicates an increase of film thickness with electrolysis time. Also, it is observed that corrosion potential suffers a shift to more positive values; the most noble electrode potential was achieved for films grown by prolonged electrolysis (15 min). Comparing 0.589 and 0.190 μAcm^{-2} values of corrosion current it can be found that it is an evident difference in corrosion behavior of samples deposited at different polarization (-0.2 and -0.15 V) by keeping constant both temperature (50^0C) and time of electrolysis (10 min). Relative to the influence of temperature the increase of corrosion current from 0.190 to 0.695 μAcm^{-2} suggest a more porous bismuth selenide film grown at 65^0C compared with that at 50^0C maintaining similar electrolysis variables (-0.15 V polarization, 10 min electrolysis time).

Table 1. The calculated corrosion parameters (corrosion current, corrosion potential, polarization resistance) in 0.5M NaCl solution for electrodeposited Bi_2Se_3 films grown on

Pt from ChCl-MA + 5 mM Bi_2O_3 + 7.5 mM SeO_2 electrolyte.

Electrodeposition variables			Corrosion parameters			
			From Tafel procedure		From linear polarization plot	
Temperature, ^{0}C	$E_{deposition}$, V	Electrolysis time, s	i_{corr}, μAcm^{-2}	E_{corr}, V	$Rp\times10^{-5}$, $k\Omega cm^2$	i_{corr}, μAcm^{-2}
50	-0.2	300	1.01	-0.268	1.92	0.97
		600	0.59	-0.242	3.78	0.24
		900	0.20	-0.160	7.80	0.12
	-0.15	600	0.19	-0.372	7.45	0.24
65	-0.15	300	1.14	-0.321	2.98	1.46
		600	0.69	-0.243	2.78	0.76
		900	0.57	-0.170	1.77	0.39

Table 1 also shows corrosion currents calculated from polarization resistance in a similar order as from Tafel procedure, although in some cases, different values were obtained for the same specimen using both procedures.

4. Conclusions

Bismuth selenide is successfully electrodeposited on platinum from an ionic liquid based on choline chloride and malonic acid mixture. At higher selenium concentrations it is suggested that selenium UPD plays an important role in Bi_2Se_3. AFM data indicate the formation of ordered spherical nanoparticles of bismuth selenide, with an average roughness of about 70 nm. Corrosion studies in 0.5M NaCl show a good resistance, which is higher for Bi_2Se_3 samples grown at lower temperatures, possibly due to a more porous structure for Bi_2Se_3 grown at higher temperatures.

Acknowledgment

Authors recognise financial support from the European Social Fund through POSDRU/89/1.5/S/54785 project: “Postdoctoral Program for Advanced Research in the field of nanomaterials”.

References

[1] S.K. Mishra, S. Satpathy, O. Jepsen, J. Phys.: Condens. Matter **9**, 461 (1997).
[2] B.R. Sankapal, R.S. Mane, C.D. Lokhande, Mater. Chem. Phys. **63**, 230 (2000).
[3] C.D. Lokhande, B.R. Sankapal, R.S. Mane, H.M. Pathan, M. Muller, M. Giersig, V. Ganeshan, Appl. Surf. Sci. **187**, 108 (2002).
[4] A. Al Bayaz, A. Giani, A. Foucaran, F. Pascal-Delannoy, A. Boyer, Thin Solid Films **441**,1 (2003).
[5] B. Pejova, I. Grozdanov, A. Tanusevski, Mater. Chem. Phys. **83** (2-3), 245 (2004).
[6] T.E. Manjulavalli, T. Balasubramanian, D. Nataraj, Chalcog. Lett. **5**, 297 (2008).
[7] L. Meng, H. Meng, W. Gong, W. Liu, Z. Zhang, Thin Solid Films **519** (22), 7627 (2011).

[8] A.P. Torane, C.D. Lokhande, P.S. Patil, C.H. Bhosale, Mater. Chem. Phys. **55** (1), 51 (1998).
[9] A.P. Torane, C.H. Bhosale, Mater. Res. Bull. **6**, 1915 (2001).
[10] J.D. Desai, Bull. Electrochem. **15**, 315 (1999).
[11] F. Xiao, C. Hangarter, B. Yoo, Y. Rheem, K-H. Lee, N.V. Myung, Electrochim. Acta, **53**, 8103 (2008).
[12] S. Subramanian, D.P. Padiyan, Mater. Chem. Phys. **107** (2-3), 392 (2008).
[13] H. Kose, M. Bicer, C. Tutunoglu, A.O. Aydin, I. Sisman, Electrochim. Acta **54**, 1680 (2009).
[14] C. Xiao, J. Yang, W. Zhu, J. Peng, J. Zhang, Electrochim. Acta **54**, 6821 (2009).
[15] S. Ham, S. Jeon, M. Park, S. Choi, K.J. Paeng, N. Myung, K. Rajeshwar, J. Electroanal. Chem. **638** (2), 195 (2010).
[16] X.L. Li, K.F. Cai, H. Li, L. Wang, C.W. Zhou, Int. J. Miner. Metall. Mater. **17** (1), 104 (2010).
[17] I. Sisman, M. Bicer, J. Alloys Comp. **509**, 1538 (2011).
[18] H. Peng, J. Zhou, D. Tang, Y. Lai, F. Liu, J. Li, Y. Liu, Electrochim. Acta **56**, 5085 (2011).
[19] F. Golgovici, A. Cojocaru, M. Nedelcu, T. Visan, J. Electron. Mater. **39** (9),2079 (2010).
[20] F. Golgovici, A. Cojocaru, L. Anicai, T. Visan, Mater. Chem. Phys. **126** (3), 700 (2011).
[21] F. Golgovici, T. Visan, Chalcog. Lett., **8**, 487 (2011).
[22] F. Golgovici, T. Visan, Chalcog. Lett. **9** (4), 165 (2012).
[23] F. Golgovici, T. Visan, Chalcog. Lett. **9** (10), 427 (2012).
[24] C. Agapescu, A. Cojocaru, F. Golgovici, A.C. Manea, A. Cotarta, Rev. Chim. (Bucharest) **63**, 911 (2012).
[25] O. Ciocirlan, O. Iulian, O. Croitoru, Rev. Chim. (Bucharest) **61** (8), 721 (2010).
[26] C. Agapescu, A. Cojocaru, A. Cotarta, T. Visan, Chalcog. Lett. **9** (10), 403 (2012).
[27] Y-C. Fu, Yu-Z. Su, H-M. Zhang, J-W. Yan, Z-H. Xie, B-W. Mao, Electrochim Acta, **55** (27), 8105 (2010).
[28] G. Torsi, G. Mamantov, J. Electroanal Chem. **30** (2), 193, (1971).
[29] P. K. Wrona, Z. Galus, Electrochim. Acta **25** (4), 371, (1980).
[30] C. Agapescu, A. Cojocaru, A. Cotarta, T. Visan, J. Appl. Electrochem. 10.1007/s10800-012-0487-0, (2012)
[31] N. Perez, Electrochemistry and Corrosion Science, Kluwer Academic Publishers, Boston, 2004, p. 100.